

An Electromagnetic Study of the Impact of Brain Anatomy on Deep Brain Stimulation

S Muñoz^{1*}, J García-Prieto², R Bajo^{3,5}, P Antoranz¹, S Ronda¹, VM Barragán¹, JC Jiménez⁴ and A Sanchis⁵

¹Department of Structure of Matter, Thermal Physics and Electronics, Complutense University of Madrid (UCM), Madrid, Spain

²Athinoula A. Martinos Center for Biomedical Imaging, Massachusetts General Hospital, Harvard University, Boston, USA

³Electrical Engineering and Bioengineering Group (EE&B), Departamento de Ingeniería Industrial, Universidad de La Laguna, La Laguna, Tenerife, Spain

⁴Department of Applied Physics in Aeronautical and Naval Engineering, ETSIAE, Polytechnic University of Madrid (UPM), Madrid, Spain

⁵Radioprotection Service, National Centre of Environmental Health, Institute of Health Carlos III, Madrid, Spain

*Corresponding Author: S Muñoz, Department of Structure of Matter, Thermal Physics and Electronics, Complutense University of Madrid (UCM), Madrid, Spain.

DOI: 10.31080/ASMS.2023.07.1589

Received: April 24, 2023

Published: June 08, 2023

© All rights are reserved by S Muñoz, et al.

Abstract

An electromagnetic simulation was performed to assess the volume of tissue activated on deep brain stimulation for two patients randomly selected. The finite element method is used to calculate the electric field distribution that predicts the volume of tissue activated. High-resolution magnetic resonance images are utilized to create patient-specific anatomical models of the subthalamic nucleus and the internal pallidum. The results confirmed the influence of brain anatomy leading to different shape and volume of tissue activated despite similar technical features. Thus, a patient-specific model and an adequate choice of stimulation parameters are crucial on deep brain stimulation outcomes.

Keywords: Finite Element Modeling; Deep Brain Stimulation; MRI Human Brain Model; Volume Tissue Activated; Subthalamic Nucleus

Introduction

Deep Brain Stimulation (DBS) is a well-known established therapy [1] for the treatment of various neurological diseases, cognitive disorders [2] and effective in the treatment of psychiatric disorders as well. The basis of this therapy is well-established on the precise implantation of an internal neuronal stimulation within the target area, specific for each neurological disorder. Despite the general effectiveness of DBS, many relevant factors can

influence the clinical response to the surgery, such as: the patient-specific anatomy, the anatomical target selected and the choice of both electrode geometry and stimulation parameters. Thus, many questions remain about possible benefits and difficulties observed on some patients, which allow in some of them, a significant reduction of medication, whereas others patients require additional medical treatment or even a new surgery. A previous quantitative assessment of the volume and shape of the VTA, might

guide a specific stimulation type and parameters (magnitude, frequency, pulse width) for each patient. So, the stimulation would be guaranteed only in the desired target avoiding side effects that may derive in future adverse consequences.

Electromagnetic simulations have become an important research field in recent years as an adequate support for the presurgical consideration of the stimulation parameters by the neurologist. In particular, the finite element technique has extensively used to predict either the voltage [3,4] or the electric field distribution [5-7]. Regarding to DBS stimulation, the most popular computational model for predicting the effects in stimulation is the volume of tissue activated for immediate translation to clinical applications. The integration of a realistic 3D MRI head model within finite element models are crucial to a quantitative understanding of the neural response of the patient. In addition, other factors influence the response to DBS such are: electrode geometry, anatomical target selected for stimulation, optimal anatomical location of the electrodes within the target or technical stimulation parameters. The goal of a DBS simulation model would be to perform an integrated analysis of these multiple data collection from neuroimaging, neuroanatomy and neurostimulation to predict the VTA during DBS on a patient-specific basis. Several studies in the literature have predicted the effects of DBS by using simulation models, with a relevant contribution to shed light on the foundation on the importance of these crucial factors of stimulation. For instance, the usefulness of a patient-specific head model to predict and visualize the VTA on specific DBS targets as the subthalamic nucleus (STN) or the internal pallidum (IP) has been extensively probed [3,8]. For instance, some studies considered a 3D MRI head model to evaluate the VTA [9-11], and others analyzed possible effects by changes on stimulation parameters [12-14] such are: alternative waveforms [15,16], the amplitude level, the stimulation frequency [17] or the pulse wide [18]. These previous studies outline aspects, that can lead to a better efficiency of DBS, regarding the technical features of DBS stimulation. Furthermore, the impedance tissue specific for each patient or technical features of the electrodes such are: the geometry [19], the orientation [20-25], the polarization or the impedance [26], are also achieved to improving efficiency in DBS therapy.

In this study, our challenge is a validation of a computational modeling to compare the effect of DBS on two different patients so that the lead location and stimulation parameters interact in a complex way leading to a specific stimulation profile for each patient. Although computational modeling has already been proved as a useful tool for estimating the effects of stimulation on an individual patient basis, to the best of our knowledge, no study has performed an interleaving simulation to analyze the effects of the relevant factors involved on DBS simultaneously. Thus, we propose an electromagnetic simulation that enables the integration of a 3D head model and the complete stimulation parameters. To address this task, we have calculated the volume and shape of the VTA on two of the main DBS targets: the subthalamic nucleus (STN) and the internal part of the pallidum (IP) for two patient-specific 3D MNI models, denoted as patient A (the male patient) and patient B (the female patient) from here on out. The advantage of our approach is twofold: firstly, it may provide a description of VTA showing a new relevant parameter: the maximal radial distance and secondly, it accommodates the choice of the technical features involved on DBS systems applicable to any target or any patient. Moreover, the different factors involved on DBS such are: electrode geometry and location, target, technical parameters and the 3D MRI head model, jointly influence the final response, often with opposite effects. From this perspective, our study proposes a holistic approach. The aim is to obtain a 3D model for a stimulation system that allows the modelling of the system as a whole, capable of providing realistic predictions about the impact of any parameter of the system on the tissue activated, but considering its interaction with all the other parameters. Thus, this approach may aim to answer the different outcomes of this therapy with similar stimulation parameters and may complement previous contributions in early untreated Parkinson's diseases [27].

Methods

3D MNI head model

Two human brains were randomly selected, a male and a female [10]. Data used in the preparation of this work were obtained from the Human Connectome Project (HCP) database. The HCP project (Principal Investigators: Bruce Rosen, M.D., Ph.D., Martinos Center at Massachusetts General Hospital; Arthur W. Toga, Ph.D., University of Southern California, Van J. Weeden, MD, Martinos Center at Massachusetts General Hospital) is supported by the

National Institute of Dental and Craniofacial Research (NIDCR), the National Institute of Mental Health (NIMH) and the National Institute of Neurological Disorders and Stroke (NINDS). HCP is the result of efforts of co-investigators from the University of Southern California, Martinos Center for Biomedical Imaging at Massachusetts General Hospital (MGH), Washington University, and the University of Minnesota. The images set consists of a high resolution MPRAGE T1 sequence and a T2 (Tr/Te = 2530/1.15 ms; TI = 1100 ms; Flip Angle = 7.0deg; FOV = 256X256 mm; 1mm isotropic voxels; BW = 651 Hz/Px; iPAT = 2; and complete acquisition time of 6 minutes). MNI fiducial points were manually identified in the T1 image and the volume was transformed into MNI space. Both images were automatically co-registered and segmented with the well-known Free Surfer [28] "recon-all --all" pipeline. Raw Free Surfer volume surfaces, defined through a set of triangles (with vertices and faces) were manually edited, both to solve singularities in them like triangle intersections or isolated vertices, and importantly to join surfaces from different hemispheres. Final head model consisted of a set of 5 self-enclosing volume surfaces: scalp, skull, gray matter, white matter and ventricles (both lateral and third and fourth ventricles), segmentations are a set of high-definition surfaces. Segmentation results can be seen in figure 1.

Figure 1: Segmentation results and the 3D Brain model for both patients studied.

Electrode models

We focused on the volume and shape of VTA using two different electrode geometries: the standard bipolar and a segmented one. On one hand we chose the 3389 quadripolar DBS lead, Medtronic, Inc. It is a platinum-iridium electrode with four cylindrical contacts of height 1,5 mm and a spacing of 0,5mm between each contact. The electrode lead and contacts have a diameter of 1,27 mm. In

this study bipolar and unipolar stimulation were considered. For bipolar electrode stimulation, the first electrode contact (labeled as 1) was grounded and the second one (2) was set to stimulation. Likewise, for unipolar electrode configuration, the second one keeps as active on stimulation, whereas a plain circle at the outer of the brain model was set as ground.

Furthermore, we chose as the directional electrode, the 8-contact directional DBS Lead™ from Boston Scientific. It is a platinum-iridium electrode with rows of contacts that are segmented circumferentially to provide both axial and rotational stimulation selectivity with an axial spacing of 0,5mm between contacts. The outer diameter of each directional lead is 1,3 mm. For this segmented electrode model, we have chosen the contacts labeled as 4, 7 and 6, to simulate respectively unilateral and bilateral stimulation. The contact 4 was grounded for both configurations, whereas the contacts (6 and 7) are set to active stimulation. The segmented contact surface area is of 1,5 mm² and an overall length of 40 cm. Both electrode geometries are shown in figure 2.

Figure 2: Electrode models considered in the study: a) Medtronic, lead nº 3389 model, 1 and 2 denote the right-electrode contacts used for bipolar and unipolar stimulation respectively. and b) Directional 8-contact segmented lead (Boston Scientific's Vercise Cartesia) with the contacts (4, 7 and 6) labeled, used for unilateral and bilateral stimulation respectively.

These systems were located at the MNI coordinates for our targets: the STN and IP [25]. In particular, the position of the stimulation electrode in the patient was just medial to the target selected, STN or GPI, as defined by the 3D Brain atlas. Thus, the coordinates were (-21,8, -10,5, -3,5) [mm] for GPI and (-9,3, -17, -1) [mm] for STN [29].

Electromagnetic simulation

We have performed an electromagnetic simulation based on the finite element technique. For this purpose, we solve the Maxwell’s equations in our model. The equations derived for electric potential with its boundary conditions were solved using the AC/DC module available in commercial Comsol Multiphysics® software package (Comsol Inc., Burlington, MA, USA). The time-dependent equation of potential was solved using the Electric Current Interface and the Pardiso Solver. Based on the resulting potential field, we calculated the electric field and the current density in the different media of the model, these quantities are crucial to assess the volume of tissue activated.

The final 3D head models were imported into Comsol Multiphysics as “stl” files. The electrode systems were designed in Comsol and were considered as terminals, voltage or current according to the stimulation considered, and the outward of the head model was set as a normal current density condition. The boundary conditions applied to the electrode surfaces were perfect conductors and insulating for contacts and lead respectively.

We created a customized mesh for our model. In order to generate a precise description of the electric field distribution along the model, each tetrahedron must occupy a region that is small enough for the electric field value to be adequately interpolated from the nodal values. Therefore, there is a compromise between the size of the finite element mesh, the level of accuracy and computing resources. Due to the fact that the dimensions involved in the different parts of the brain are different, an adaptative mesh was created so that the size of the basic tetrahedron is varied for the different regions. Therefore, in order to obtain an accurate result for the electric field within the white and grey matter, the number of tetrahedra in these regions had to be considerably higher (500000) than the corresponding number for the region occupied by scalp (12000).

In this study both electrode models were simulated to operate in voltage and current mode. First of all, we consider the typical stimulation by using a train of impulses of 130 Hz, 60 ms, and a voltage of 3.5V. Recent studies [21] demonstrated that directional DBS emerged to increase the therapeutic window and may guide postoperative programming. Furthermore, both systems have also

operated with a current source at an intensity of 50 µA, a value selected to be therapeutic but below the threshold intensity for contralateral forepaw dyskinesia [30]. The current stimulation presents as advantage that the total current is independent from the variations in brain tissue impedance. Thus, it may be interesting to compare the influence of brain’s anatomy on both voltage and current stimulation.

These technical features are in good agreement with previous studies [15,31,32] that reviewed and compared technical features of different DBS systems. So, lower amplitudes and smaller pulse widths or even other alternative waveforms may lead to more effective outcomes. Thus, we include for comparison a lower amplitude value of 1 V and a train of impulses of 40 ms and 100 ms [33]. In addition, three alternative waveforms, triangular, sinusoidal and sawtooth were considered.

To solve the time-dependent equations we need the electrical properties of the different media of the model. At low frequency, as typically used in DBS, the different head tissues may be considered as purely resistive. Thus, the main contribution to the current density through the different brain layers is the tissue’s conductivity whereas the contribution of the dielectric permittivity is negligible. First, we performed a simulation isotropic and therefore each tissue was characterized by a constant value of conductivity that represents the mean value for each tissue reported in the literature for simple brain models [34] and the conductive material for the electrodes. Table 1 shows the conductivity values considered.

Tissue	Conductivity (S/m)
Electrode contacts	8.9x10 ⁶
Electrode lead	1x10 ⁻¹²
Grey Matter	0.4
Scalp	0.44
Skull	0.006
Vents	1.79
White Matter	0.18

Table 1: Values of conductivity considered in the simulation.

The region close to the electrodes behaves as an inhomogeneous conductor that accounts for the tissue healing specific for each patient and the effects of the electrode impedances. Butson., *et*

al. [35] studied the effect that the electrical properties of the 3D tissue surrounding the electrodes have on the VTA. So, they concluded that a 500 mm thick encapsulation layer characterized by a conductivity value of 0,07 S/m, may account for these effects. So, in this study we considered a cylinder of a radius of 0,5 mm surrounding the electrodes with a conductivity value of 0.07S/m.

Despite isotropic simulations may provide qualitative response for the effects on the VTA shape, the effects of tissue heterogeneity and anisotropy are crucial on the electric field distribution and therefore on the VTA. In this study we focused on the anisotropy of the skull and the white matter. Thus, grey matter and cerebrospinal fluid are assumed to be homogeneous and isotropic so an average value frequency independent is often reported. For example, for the grey matter, Logothetis, *et al.* [36] reported an average value of 0,404 S/m which is essentially frequency independent in the range from 1 Hz to 10 kHz. Previous studies reported measurements of the CSF conductivity with a constant and mean value about 1,7S/m [37], [38], we have chosen a constant value of 1.79 S/m in this study. However, white matter is much more anisotropic and less homogeneous than gray matter. Its longitudinal conductivity may be from 5 to 10 times greater than its transverse conductivity. Thus, a separate value for longitudinal and transverse conductivity is often reported. For example, Nicholson [39] reported average transverse and longitudinal conductivity values of 0.13 S/m and 1.13 S/m.

Despite the heterogeneous nature of the scalp, a typical value of 0.44 S/m [34] is often considered. Finally, the skull presents a conductivity not uniform due not only to the different layers but also to the variation of its thickness with a crucial role of the brain to skull conductivity value. In our isotropic model we consider a conductivity ratio value of 50:1 as typically reported [40]. However, lower values of brain to skull conductivity ratio are considered in this study so recently new studies [41] indicated that this value may lie in the range between 20:1 and 50:1. We analyze the effect of changes of the ratio values in the range from 20:1 to 50:1 on the VTA due mainly to changes on the brain conductivity.

Results

We determined the effect of both electrode geometry and stimulation parameters on the VTA for both patients during voltage

and current controlled DBS. Previous studies [42] determined the threshold activation value for voltage and current stimulation, fixed at 26.67 V/cm² and 54.3 μA/cm² respectively. These threshold values were used to create isosurfaces to predict the shape and volume of the VTA generated for a value one percent higher than the threshold values for voltage and current. Figure 3 shows, as example for patient A, a vertical cross section of the 3D head model, with the VTA distribution at STN for the three electrode geometries.

Figure 3: Vertical cross section of the 3D head model generated at STN for subject A.

The results confirmed a VTA shape axially symmetrical around the activated contacts for bipolar stimulation. However, both directional electrodes formed an elliptical profile along the length of the lead. Nonetheless the bilateral stimulation divides the VTA between both sides of the electrodes while the unilateral stimulation keeps all volume only at one side but both revealed the loss of the axial symmetry around contacts.

As mentioned, two subjects (A and B) were studied, each in two different brain regions (IP and STN). Three different types of electrodes were used (bipolar and segmented with unilateral and bilateral stimulation). The signal was configured with a train of pulses, with the following parameters: 130 Hz, 60μs, a voltage of 3.5V, and a rectangular shape. Subsequently, the following simulations were performed, obtaining following results.

Variation of the voltage of the train pulse used and current stimulation

With all parameters set to the values just mentioned, three different voltages (1V, 2V, and 3.5V) were used. As can be seen in the Figure 4, the results confirmed similar VTA shapes for both

subjects, the VTA value decreases as the voltage decreases, for all three types of electrodes (with the exception of subject A in the STN region), and in both studied regions. Higher values were obtained for subject B with bipolar stimulation at both targets whereas unilateral and bilateral stimulation led to higher values for subject. The subject B exhibits significant differences between both electrode geometries. The results for the subject A also confirmed differences between the different stimulations but are less significant. It should also be emphasized that the differences between both targets under unilateral and bilateral stimulation were hardly noticeable for both patients.

As mentioned before, a current stimulation was also performed. The results showed for subject A, higher VTA values about ten times in comparison to voltage simulation for bipolar configuration at both targets. However, the unilateral configuration led to lower values of VTA. The values obtained for subject B were always significant lower for both configurations and leading to more significant differences between the three electrode models studied.

In our study, we focused on a new parameter, the radial distance from the contacts. The calculus of the radial distance from contacts may be of great importance to assure the spread of stimulation area. Thus, its overlap with specific brain regions may be seen. The most significant differences were obtained for subject A for both voltage and current stimulation and targets. The values were also higher for current stimulation



Variation of the pulse width introduced

Now, as in the previous section, with all initial parameters set to the mentioned values, the pulse width used was varied from 40 μs to 100 μs (in 5 μs steps). No relevant variations were observed in the obtained VTA values.

Variation of the input frequency

In this case, for the same described parameters, simulations were performed with two different input frequency values: 100 Hz and 130 Hz. The following results were obtained (see Figure 5).



Figure 5: Above: Variation of VTA and Below: Variation of Radial distance as a function of the two introduced frequencies (100 Hz and 130 Hz).

As can be seen in both cases, the VTA for the bipolar electrode increases as the frequency decreases. However, for the other two electrodes (unilateral and bilateral), in subject A, the VTA decreases as the frequency decreases, and in subject B, the VTA remains constant with the decrease in frequency. Significant differences were obtained for subject B for the radial distance at highest frequency at both targets.

Variation of the waveform of the introduced signal

Here, with all initial parameters mentioned, simulations were performed for three different signal shapes: sinusoidal, triangle, and sawtooth. The following results were obtained for the VTA (see Figure 6).

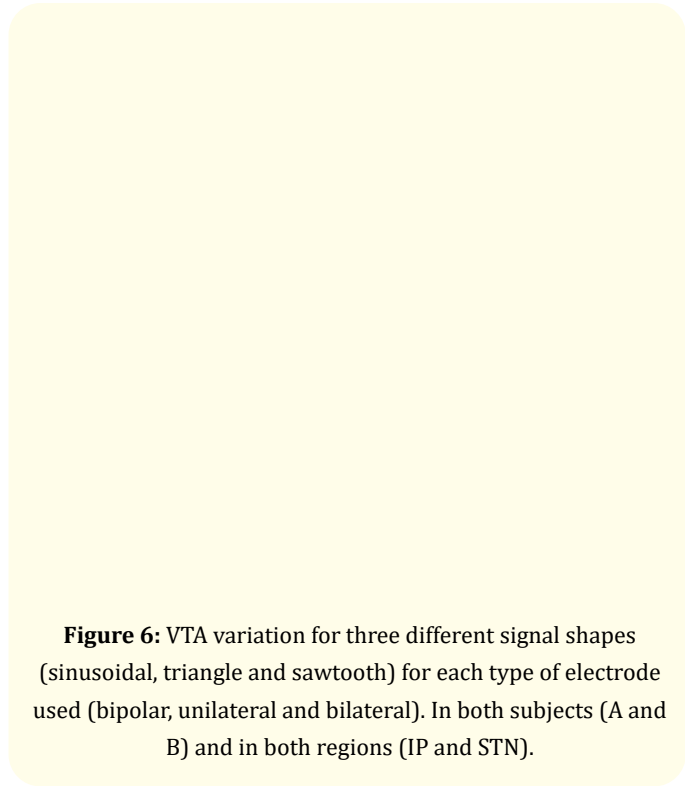


Figure 6: VTA variation for three different signal shapes (sinusoidal, triangle and sawtooth) for each type of electrode used (bipolar, unilateral and bilateral). In both subjects (A and B) and in both regions (IP and STN).

As the Figure shows, the highest VTA value was obtained for the “triangle” signal shape. In subject A, this was higher for the bilateral electrode, and in subject B, it was clearly higher for the bipolar electrode.

Variation of the conductivity ratio between brain and skull

This simulation was also carried out with the same initial parameters, but we only found differences for subject A and in the

IP region. The conductivity ratio was varied in the range from 20:1 to 50:1 by changing the brain conductivity. The results obtained showed higher VTA values as the conductivity ratio increases, with differences of about a 30% between the lowest and the highest value of the ratio considered.

Discussion and Conclusion

Despite the potential major impact of DBS on neuroscience research, the modulation of the specific tissue activated for each patient, optimizing the totality of the stimulation parameters, has rarely been studied. Previous studies assessed the volume of tissue activated for different electrode geometries or changes of the main technical features. In the present study, we confirm that the patient' anatomy has a crucial role in modulating the tissue activated for similar technical features.

In the present study it is investigated the effects of different parameters on the volume of tissue activated (VTA) using three types of electrodes (bipolar and segmented with unilateral and bilateral stimulation) and a pulse train signal with fixed parameters (130 Hz, 60 μ s, 3.5V, rectangular). Two subjects (A and B) were studied in two different brain regions (IP and STN), and simulations were performed using the commercial software Comsol. The first simulation examined the relationship between voltage and VTA, and the possible effect that voltage variation can produce on the VTA. Three different voltages (1V, 2V, and 3.5V) were applied to the electrodes. The results showed that decreasing the voltage led to a decrease in the VTA for all electrode types except for subject A in the STN region. This effect was observed in both regions studied. These results are in line with what has been observed in previous studies [43,44], in which it is stated that an increase in voltage leads to an increase in VTA. The results also confirmed the influence of brain anatomy to assess the differences between voltage and current stimulation. In addition, the new parameter considered in this study, the radial distance, allowed to distinguish similar volumes but with different shapes.

The next simulation investigated the effect of pulse width on the VTA, with pulse widths ranging from 40 μ s to 100 μ s. No significant changes in the VTA were observed with varying pulse widths. Thus, we did not find evidence about the possible influence that the width of the pulse used may have on the size of the VTA. It seems that it is not a relevant parameter in said volume.

The third simulation examined the effect of frequency on the VTA, with two different frequencies (100 Hz and 130 Hz) applied to the electrodes. The results showed that the VTA increased with decreasing frequency for the bipolar electrode in both subjects, while for the other two electrodes (unilateral and bilateral), the VTA decreased with decreasing frequency in subject A and remained constant in subject B. One of the most relevant factors of the stimulation is the frequency. This study shows that a low frequency stimulation may have opposite effects.

Also, we investigated the effect of signal waveform on the VTA, with three different waveforms (sinusoidal, triangle, and sawtooth) applied to the electrodes. Although there are some studies [45] indicating that the VTA was significantly larger with sinusoidal wave stimulation compared to triangular or sawtooth wave stimulation. Here, our results showed that the triangle waveform produced the highest VTA values, with the bilateral electrode producing higher VTA values in patient A and the bipolar electrode producing higher VTA values in patient B. From our point of view, this demonstrates that it is necessary to carry out more studies in this regard, which allow elucidating whether the waveform used has an effect on the VTA or not, and if so, determine exactly what it is.

Finally, the effect of the conductivity ratio between the brain and skull was investigated in subject A in the IP region. The results showed that increasing the conductivity ratio led to an increase in the VTA. These results are in agreement with works such as those by [8,46], who suggested that the brain-skull conductivity ratio may influence the size and shape of the VTA in deep brain stimulation. They indicated that a higher brain-skull conductivity ratio is related to a larger VTA on DBS.

All these simulations demonstrate that various parameters, including voltage, frequency, waveform, and conductivity ratio, can significantly impact the VTA in different electrode configurations and brain regions. These findings could have important implications for the design and optimization of deep brain stimulation protocols for clinical applications. Combination of patient-specific anatomy and stimulation parameters shows to be a valid approach to predict the volume and shape of VTA. Despite our investigation is only limited to two patients, the observed variations confirmed that may be helpful to replicate our research in datasets including a large number of patients. This

approach might lay the foundation for technological challenges and future developments in neurostimulation complementing previous contributions in this issue [47].

Acknowledgments

Financial support from Santander UCM Research (project PR41/17-21015) is gratefully acknowledged.

Data were provided by the Human Connectome Project, WU-Minn Consortium (Principal Investigators: David Van Essen and Kamil Ugurbil; 1U54MH091657) funded by the 16 NIH Institutes and Centers that support the NIH Blueprint for Neuroscience Research; and by the McDonnell Center for Systems Neuroscience at Washington University.

Bibliography

1. A L Benabid., *et al.* "Chronic electrical stimulation of the ventralis intermedius nucleus of the thalamus as a treatment of movement disorders". *Journal of Neurosurgery* (1996).
2. M Meinzer., *et al.* "Electrical brain stimulation improves cognitive performance by modulating functional connectivity and task-specific activation". *Journal of Neuroscience* 32.5 (2012): 1859-1866.
3. M Åström., *et al.* "Method for patient-specific finite element modeling and simulation of deep brain stimulation". *Medical and Biological Engineering and Computing* 47.1 (2009): 21-28.
4. S Miocinovic., *et al.* "Experimental and theoretical characterization of the voltage distribution generated by deep brain stimulation". *Experimental Neurology* 216.1 (2009): 166-176.
5. A Chaturvedi., *et al.* "Patient-specific models of deep brain stimulation: Influence of field model complexity on neural activation predictions". *Brain Stimulation* 3.2 (2010): 65-77.
6. C R Butson and C C McIntyre. "The Use of Stimulation Field Models for Deep Brain Stimulation Programming". *Brain Stimulation* 8.5 (2015): 976-978.
7. G Duffley., *et al.* "Evaluation of methodologies for computing the deep brain stimulation volume of tissue activated". *Journal of Neural Engineering* 16.6 (2019).
8. C R Butson., *et al.* "Patient-specific analysis of the volume of tissue activated during deep brain stimulation". *Neuroimage* 34.2 (2007): 661-670.
9. A Nowacki., *et al.* "Accuracy of different three-dimensional subcortical human brain atlases for DBS -lead localisation". *NeuroImage Clinics* 20 (2018).
10. DC Van Essen., *et al.* "The Human Connectome Project: A data acquisition perspective". *NeuroImage* (2012).
11. A Horn. "The impact of modern-day neuroimaging on the field of deep brain stimulation". *Current Opinion in Neurology* 32.4 (2019).
12. T M Herrington., *et al.* "Mechanisms of deep brain stimulation". *Journal of Neurophysiology* 115.1 (2016).
13. M Picillo., *et al.* "Programming Deep Brain Stimulation for Tremor and Dystonia: The Toronto Western Hospital Algorithms". *Brain Stimulation* 9.3 (2016).
14. A Ramirez-Zamora., *et al.* "Proceedings of the Sixth Deep Brain Stimulation Think Tank Modulation of Brain Networks and Application of Advanced Neuroimaging, Neurophysiology, and Optogenetics". in *Frontiers in Neuroscience* (2019): 13.
15. K Argiti., *et al.* "Deep brain stimulation: increasing efficiency by alternative waveforms". *Current Directions in Biomedical Engineering* 2.1 (2016): 145-148.
16. S F Lempka., *et al.* "Characterization of the stimulus waveforms generated by implantable pulse generators for deep brain stimulation". *Clinical Neurophysiology* 129.4 (2018).
17. Y Shon., *et al.* "High frequency stimulation of the subthalamic nucleus evokes striatal dopamine release in a large animal model of human DBS neurosurgery". *Elsevier* (2010).
18. F Steigerwald., *et al.* "Pulse duration settings in subthalamic stimulation for Parkinson's disease". *Movement Disorder* 33.1 (2018).
19. U Gimsa., *et al.* "Matching geometry and stimulation parameters of electrodes for deep brain stimulation experiments - Numerical considerations". *Journal of Neuroscience Methods* 150.2 (2006): 212-227.
20. A Hellerbach., *et al.* "DiODE: Directional orientation detection of segmented deep brain stimulation leads: A sequential algorithm based on CT imaging". *Stereotactic and Functional Neurosurgery* 96.5 (2018).

21. TA Dembek, *et al.* "Directional DBS leads show large deviations from their intended implantation orientation". *Parkinsonism and Related Disorders* 67 (2019).
22. L J Bour, *et al.* "Directional recording of subthalamic spectral power densities in Parkinson's disease and the effect of steering deep brain stimulation". *Brain Stimulation* 8.4 (2015).
23. L J Lehto, *et al.* "Orientation selective deep brain stimulation". *Journal of Neural Engineering* 14.1 (2017).
24. A Husch, *et al.* "PaCER - A fully automated method for electrode trajectory and contact reconstruction in deep brain stimulation". *NeuroImage Clinics* 17 (2018).
25. TA Dembek, *et al.* "Directional DBS increases side-effect thresholds—A prospective, double-blind trial". *Movement Disorder* 32.10 (2017).
26. C Butson C MC. neurophysiology, and undefined 2005. "Tissue and electrode capacitance reduce neural activation volumes during deep brain stimulation". Elsevier (2005).
27. J Rusz, *et al.* "Automated speech analysis in early untreated Parkinson ' s disease : Relation to gender and dopaminergic transporter imaging". September (2021): 81-90.
28. B Fischl. "FreeSurfer". *Neuroimage* 62.2 (2012): 774-781.
29. F Hell, *et al.* "Deep brain stimulation programming 2.0: Future perspectives for target identification and adaptive closed loop stimulation". *Frontiers in Neurology* 10 (2019).
30. V Vedam-Mai, *et al.* "Tissue Response to Deep Brain Stimulation and Microlesion: A Comparative Study". *Neuromodulation* 19.5 (2016): 451-458.
31. M Arlotti, *et al.* "The adaptive deep brain stimulation challenge". *Parkinsonism and Related Disorders* 28 (2016).
32. A Amon and F Alesch. "Systems for deep brain stimulation: review of technical features". *Journal of Neural Transmission* 124.9 (2017).
33. J Volkmann, *et al.* "Introduction to the programming of deep brain stimulators". *Movement Disorder* 17.3 (2002).
34. P C Miranda. "Physics of effects of transcranial brain stimulation". *Handbook of Clinical Neurology* 116 (2013): 353-366.
35. C R Butson and CC McIntyre. "Role of electrode design on the volume of tissue activated during deep brain stimulation". *Journal of Neural Engineering* 3.1 (2006): 1-8.
36. NK Logothetis, *et al.* "In Vivo Measurement of Cortical Impedance Spectrum in Monkeys: Implications for Signal Propagation". *Neuron* 55.5 (2007): 809-823.
37. S B Baumann, *et al.* "The electrical conductivity of human cerebrospinal fluid at body temperature". *IEEE Transactions on Biomedical Engineering* 44.3 (1997): 220-223.
38. H McCann, *et al.* "Variation in Reported Human Head Tissue Electrical Conductivity Values" 32.5 (2019).
39. P W Nicholson. "Specific impedance of cerebral white matter". *Experimental Neurology* 13.4 (1965): 386-401.
40. Y Zhang, *et al.* "Estimation of in vivo brain-to-skull conductivity ratio in humans". *Applied Physics Letters* 89.22 (2006).
41. V J, *et al.* "In vivo measurement of the brain and skull resistivities using an EIT-based method and realistic models for the head". *IEEE Transactions on Biomedical Engineering* 50 (2003): 754-767.
42. A M Lozano, *et al.* "Deep brain stimulation for Parkinson's disease: Disrupting the disruption". *Lancet Neurology* 1.4 (2002): 225-231.
43. C C McIntyre, *et al.* "Cellular Effects of Deep Brain Stimulation: Model-Based Analysis of Activation and Inhibition". *Journal of Neurophysiology* 91.4 (2004): 1457-1469.
44. A Chaturvedi, *et al.* "Artificial neural network based characterization of the volume of tissue activated during deep brain stimulation". *Journal of Neural Engineering* 10.5 (2013).
45. M Alcauskas, *et al.* "Write Click: Editor ' s Choice" (2013).
46. B Howell, *et al.* "A Driving-Force Predictor for Estimating Pathway Activation in Patient-Specific Models of Deep Brain Stimulation". *Neuromodulation* 22.4 (2019): 403-415.
47. A M Lozano, *et al.* "Deep brain stimulation: current challenges and future directions". *Nature Reviews Neurology* 15.3 (2019): 148-160.